



2-15-2002

## A Peptide Analogue to a Fusion Domain Within Photoreceptor Peripherin/rds Promotes Membrane Adhesion and Depolarization

Kathleen Boesze-Battaglia  
*University of Pennsylvania*

Frank P. Stefano

Madeline Fenner

Andrew A. Napoli Jr.

Follow this and additional works at: [https://repository.upenn.edu/dental\\_papers](https://repository.upenn.edu/dental_papers)

 Part of the [Dentistry Commons](#)

---

### Recommended Citation

Boesze-Battaglia, K., Stefano, F. P., Fenner, M., & Napoli, A. A. (2002). A Peptide Analogue to a Fusion Domain Within Photoreceptor Peripherin/rds Promotes Membrane Adhesion and Depolarization. *Biochimica et Biophysica Acta - Biomembranes*, 1463 (2), 343-354. [http://dx.doi.org/10.1016/S0005-2736\(99\)00226-6](http://dx.doi.org/10.1016/S0005-2736(99)00226-6)

This paper is posted at ScholarlyCommons. [https://repository.upenn.edu/dental\\_papers/350](https://repository.upenn.edu/dental_papers/350)  
For more information, please contact [repository@pobox.upenn.edu](mailto:repository@pobox.upenn.edu).

---

## A Peptide Analogue to a Fusion Domain Within Photoreceptor Peripherin/rds Promotes Membrane Adhesion and Depolarization

### Abstract

Photoreceptor peripherin/rds promotes membrane fusion, through a putative fusion domain located within the C-terminus (Boesze-Battaglia et al., *Biochemistry* 37 (1998) 9477-9487). A peptide analogue to this region, PP-5, competitively inhibits peripherin/rds mediated fusion in a cell free assay system. To characterize how this region is involved in the fusion process we investigated two of the individual steps in membrane fusion, membrane adhesion and membrane destabilization inferred from depolarization studies. Membrane depolarization was measured as the collapse of a valinomycin induced  $K^+$  diffusion potential in model membranes, using a potential sensitive fluorescent probe, diS-C<sub>2</sub>-5. PP-5 induced membrane depolarization in a concentration dependent manner. PP-5 has been shown by Fourier transform infrared spectroscopy to be an amphiphilic  $\alpha$ -helix. Therefore, the requirement for an amphiphilic  $\alpha$ -helix to promote depolarization was tested using two mutant peptides designed to disrupt either the amphiphilic nature of PP-5 (PP-5AB) or the  $\alpha$ -helical structure (PP-5HB). PP-5AB inhibited PP-5 induced depolarization when added in an equimolar ratio to PP-5. Neither mutant peptide alone or in combination with PP-5 had any effect on calcium dependent vesicle aggregation. Using non-denaturing gel electrophoresis and size exclusion chromatography techniques PP-5 was shown to form a tetrameric complex. Equimolar mixtures of PP-5 and PP-5AB formed a heterotetramer which was unable to promote membrane depolarization. The hypothesis that PP-5 tetramers promote membrane depolarization is consistent with the calculated Hill coefficient of 3.725, determined from a Hill analysis of the depolarization data. Copyright (C) 2000 Elsevier Science B.V.

### Keywords

Membrane fusion; Peripherin/rds and fusion peptide; Photoreceptor

### Disciplines

Dentistry



ELSEVIER

Biochimica et Biophysica Acta 1463 (2000) 343–354



www.elsevier.com/locate/bba

# A peptide analogue to a fusion domain within photoreceptor peripherin/rds promotes membrane adhesion and depolarization

Kathleen Boesze-Battaglia \*, Frank P. Stefano, Madeline Fenner, Andrew A. Napoli Jr.

*Department of Molecular Biology, University of Medicine and Dentistry of New Jersey-SOM, 2 Medical Center Drive, Stratford, NJ 08084, USA*

Received 22 June 1999; received in revised form 7 October 1999; accepted 4 November 1999

## Abstract

Photoreceptor peripherin/rds promotes membrane fusion, through a putative fusion domain located within the C-terminus (Boesze-Battaglia et al., *Biochemistry* 37 (1998) 9477–9487). A peptide analogue to this region, PP-5, competitively inhibits peripherin/rds mediated fusion in a cell free assay system. To characterize how this region is involved in the fusion process we investigated two of the individual steps in membrane fusion, membrane adhesion and membrane destabilization inferred from depolarization studies. Membrane depolarization was measured as the collapse of a valinomycin induced  $K^+$  diffusion potential in model membranes, using a potential sensitive fluorescent probe, diS-C<sub>2</sub>-5. PP-5 induced membrane depolarization in a concentration dependent manner. PP-5 has been shown by Fourier transform infrared spectroscopy to be an amphiphilic  $\alpha$ -helix. Therefore, the requirement for an amphiphilic  $\alpha$ -helix to promote depolarization was tested using two mutant peptides designed to disrupt either the amphiphilic nature of PP-5 (PP-5AB) or the  $\alpha$ -helical structure (PP-5HB). PP-5AB inhibited PP-5 induced depolarization when added in an equimolar ratio to PP-5. Neither mutant peptide alone or in combination with PP-5 had any effect on calcium dependent vesicle aggregation. Using non-denaturing gel electrophoresis and size exclusion chromatography techniques PP-5 was shown to form a tetrameric complex. Equimolar mixtures of PP-5 and PP-5AB formed a heterotetramer which was unable to promote membrane depolarization. The hypothesis that PP-5 tetramers promote membrane depolarization is consistent with the calculated Hill coefficient of 3.725, determined from a Hill analysis of the depolarization data. © 2000 Elsevier Science B.V. All rights reserved.

*Keywords:* Photoreceptor; Membrane fusion; Peripherin/rds and fusion peptide

## 1. Introduction

Membrane fusion processes are essential for normal development and physiological function in all

cell types [1,2]. A commonality among most fusion processes is the mediation and regulation of these processes by unique fusion proteins (for review see [3]) which share common motifs (i.e. fusion peptide regions). A characteristic structural feature of viral fusion proteins [3] and of mammalian fusion proteins, such as fertilin [4–6] and meltrin [7], is the presence of short fusion peptides generally 16–26 amino acids in length. Such fusion peptides are often part of a membrane anchored domain and may be internal to the polypeptide chain [8]. Molecular mod-

Abbreviations: ROS, rod outer segment; LUV, large unilamellar vesicle; SUV, small unilamellar vesicle; diS-C<sub>2</sub>-5, 3,3'-diethylthiodicarbocyanine iodide; RhPP-5, rhodamine labeled PP-5

\* Corresponding author. Fax: (609) 5666232;  
E-mail: battagli@umdnj.edu

eling and biophysical studies show that some fusion peptides form amphiphilic  $\alpha$ -helical structures [9–12], while others form  $\beta$ -structures [13]. Most of these peptides are oriented obliquely within the opposing bilayer [14] and destabilize the target membrane [8,10,14–17] and/or host membranes [18–22]. In a number of fusion systems these fusion peptide regions mediate the individual steps in fusion as multimeric complexes. The precise oligomeric state of a number of these peptides has been identified; hemagglutinin (HA) induced fusion, for example, requires the cooperation of at least three HA trimers [23].

Fusion processes also play an important role in maintaining the normal structure of retinal rod cells. In the outer segment region of the cell, the coordinated processes of disk morphogenesis (at base) and disk shedding (at tip) define a program of outer segment renewal and disposal [24]. These processes maintain a stack of closed flattened membranous disks organized in a discontinuous lateral array. A step during both new disk closure and disk membrane packet formation prior to shedding requires the fusion of opposing membranes. Fusion during disk packet formation is documented in microscopic studies showing rod outer segment (ROS) vesiculation and tubulation in the region of old disks and packet formation [25–28]. An analysis of dye penetration into distinct regions of the ROS and the observation that large molecules do not enter the narrow bands of dye stained region of the ROS suggest a fusion of the plasma membrane with the disk membranes [29–31]. Fusion between these two membranes has since been modeled in cell free assay systems [32–35].

We have recently identified a candidate fusion protein, called peripherin/rds, in photoreceptor rod cells. Peripherin/rds is located within the disk rim [36], the surface that contacts and fuses with plasma membrane in disk packet formation. It is a 39 kDa integral membrane glycoprotein consisting of four transmembrane domains and two intradiskal loops [37–39]. A portion of the C-terminus (residues 294–315) is highly conserved between and within species (i.e. *Xenopus*, human, mouse, rat, bovine and chicken [40]) and at least one C-terminal serine residue is phosphorylated [33]. Within the ROS disk rim, peripherin/rds forms disulfide linked homodimers which complex non-covalently with a non-glycosylat-

ed homologue, rom-1, to form a heterotetrameric complex [41–45]. Using a cell free fusion assay system as a model of the fusion between disk rims and plasma membrane, we have shown that purified peripherin/rds promotes membrane fusion [33,34]. Fusion is mediated through at least one region of the C-terminal domain from residues 311 to 325, hypothesized to serve as a fusion peptide. We have previously shown that a peptide analogue to this region, called PP-5, inhibits fusion between ROS plasma membrane and peripherin/rds recombinants and promotes membrane adhesion and model membrane fusion [34]. This peptide is an amphiphilic  $\alpha$ -helix based on Fourier transform infrared spectroscopy (FTIR [34]), a structure consistent with that of other membrane fusion peptides [2–4].

Since biological membrane fusion is a complex series of biochemical events, attempts to understand the steps in the fusion process rely on the use of simplified model systems. Synthetic peptides that are analogous to, or closely resemble the fusion peptide regions of fusion proteins have been used extensively in model membrane studies to understand the molecular mechanism by which these regions promote fusion. Peptide analogues of HIV-1 gp41 [46,47], Sendai virus F1 [48], baculovirus GP64 [49], measles virus F1 [50], S-protein of hepatitis [51] and sperm fertilin [52] fusion peptide regions have allowed elucidation of the mechanism(s) by which these fusion proteins promote infection and fertilization.

While PP-5 has been shown to promote membrane adhesion and model membrane fusion, its role in membrane destabilization, another prerequisite step in fusion, has until now not been evaluated. In the studies described herein, PP-5 is shown to promote membrane destabilization, in the form of diffusion potential collapse, and aggregation in a dose dependent fashion. Analogous to other membrane fusion peptides, the requirement for an amphiphilic  $\alpha$ -helical structure to mediate the steps in fusion was also demonstrated with two mutant peptides designed to alter the biophysical properties of PP-5. Wild type and mutant peptide to self- and co-assembly was evaluated and the ability of PP-5 to promote membrane depolarization is discussed in the context of oligomer formation. These data provide additional and more compelling support for the identification

of this region as a fusion peptide within peripherin/rds and adds to the growing list of fusion peptides with common structural and functional properties [3].

## 2. Experimental procedures

### 2.1. Materials

Phosphatidylserine (PS, bovine brain), phosphatidylcholine (PC, egg), phosphatidylethanolamine (PE) and cholesterol used to synthesize small unilamellar vesicles (SUVs) and large unilamellar vesicles (LUVs) were purchased from Avanti Polar Lipids (Atlanta, GA). All other chemicals were purchased from Sigma (Saint Louis, MO). PP-5 corresponding to residues 311–325 in the C-terminal region of bovine peripherin/rds and mutant peptides designated PP-5HB and PP-5AB were purchased from Quality Control Biochemicals (QCB). PP-3 corresponding to residues 331–345 in the C-terminal region of bovine peripherin/rds was synthesized by QCB.

### 2.2. Membrane permeability studies

Membrane bilayer destabilization was inferred from membrane depolarization studies and measured fluorimetrically with the cation sensitive dye, diS-C<sub>2</sub>-5, as a collapse in a valinomycin induced diffusion potential in model membranes [53]. SUVs composed of phosphatidylcholine:phosphatidylserine:cholesterol in a 4:4:1 molar ratio were prepared by probe sonication in the presence of K<sup>+</sup> containing buffer (50 mM K<sub>2</sub>SO<sub>4</sub>, 10 mM HEPES-SO<sub>4</sub>, pH 6.8). An aliquot of the SUVs (phospholipid concentration = 36 nmoles) was added to 10 ml of isotonic buffer (50 mM Na<sub>2</sub>SO<sub>4</sub>, 10 mM HEPES-SO<sub>4</sub>, pH 6.8) containing 10 μl of the fluorescent probe diS-C<sub>2</sub>-5 (stock = 1 mM) and incubated at 37°C until a stable baseline fluorescence was established. The addition of valinomycin (final concentration = 10<sup>-7</sup> M), selectively permeabilized the vesicles to K<sup>+</sup>, creating a negative diffusion potential inside the vesicles resulting in the quenching of the dye's fluorescence. Peptides from a 1 mg/ml stock in either dH<sub>2</sub>O or K<sup>+</sup>-free buffer were added in 25, 75, or 100 μl aliquots. Fluorescence was recorded at λ<sub>ex</sub> = 620 nm

and λ<sub>em</sub> = 670 nm for 90 min after the addition of the various peptides. An increase in fluorescence intensity upon the addition of peptides was indicative of a dissipation of the diffusion potential due to peptide induced destabilization. To quantitate the total fluorescence recovered, fluorescence was monitored before the addition of valinomycin, following the addition of valinomycin and after the addition of the desired peptide. The percent fluorescence recovery was calculated as described previously [53], using the equation below:

$$F_t = [(I_t - I_o) / (I_f - I_o)] \times 100$$

I<sub>t</sub> is the fluorescence after the addition of the peptide, at time *t*, I<sub>o</sub> is fluorescence after the addition of valinomycin, I<sub>f</sub> = fluorescence intensity prior to the addition of valinomycin. Mellitin (final concentration = 9.0 μg/ml) was added to confirm that the increase in fluorescence observed was due to a collapse in the diffusion potential. In all of the permeability studies mellitin was able to dissipate the valinomycin induced diffusion potential after the addition of those peptides which had no effect.

### 2.3. Vesicle aggregation experiments

Change in vesicle size was monitored using UV/VIS spectroscopy essentially as described [34,53]. The SUVs were composed of PC:PS:CHOL (4:4:1) and prepared in the presence of 16 μM Ca<sup>2+</sup> [34]. Aliquots of the various peptides were added individually and in combination to SUVs as described in the figure legends. Vesicle aggregation was monitored as a change in vesicle size, detected as a change in absorbance at 380 nm, recorded every 0.1 min for 10 min. Reversible aggregation was distinguished from fusion with the addition of 1 M EDTA to a final concentration of 33 mM and the absorbance monitored for an additional 3 min. All aggregation studies were performed at 37°C.

### 2.4. Size exclusion chromatography

The oligomeric state of the peptides was determined using size exclusion HPLC, with a HR10/30 Superdex column (internal diameter 10 mm, 30 cm column length, bed volume, 24 ml; Pharmacia, Biotech), eluted with an isocratic gradient of 0.25 M

NaCl in 0.02 M Na<sub>2</sub>HPO<sub>4</sub> pH 7.40 at a flow rate of 0.25 ml/min or 0.50 ml/min as indicated. The elution was monitored at 214 nm and the individual peptide species isolated. Samples were routinely loaded onto the column in distilled water from a 1 mg/ml stock solution. The injection volumes varied from 25 to 100 µl (corresponding to 5–30 nmoles) as described in the figure legends and tables. The molecular weights of the oligomeric complexes was determined by comparison to proteins of known molecular mass (cytochrome *c* 12 500 Da, aprotinin 6500 Da, gastrin 2126 Da, substance P 1348 Da, (Gly)<sub>6</sub> 360 Da, (Gly)<sub>3</sub> 189 Da and glycine 75 Da). The various peak assignments were based on individual runs of the various peptides compared to the elution volume of the standards.

### 2.5. Peptide binding studies

The extent of peptide association with small unilamellar PS:PC:CHOL (4:4:1) vesicles was measured using a rhodamine labeled PP-5 derivative, designated RhPP-5 (sequence shown in Table 1). SUVs were added to RhPP-5 at 37°C as described by others in tryptophan binding experiments [54,55]. The rhodamine fluorescence intensity was measured as a function of increasing lipid to peptide ratio with a  $\lambda_{\text{ex}} = 560$  nm (slit width = 10) and  $\lambda_{\text{em}} = 590$  nm (slit width = 20). No change in RhPP-5 fluorescence was observed when buffer was added in amounts equal to the volume of SUVs.

### 2.6. Denaturing and non-denaturing gel electrophoresis

Peptides were separated on discontinuous denatur-

ing tricine gels containing 6 N urea and discontinuous non-denaturing tricine gels containing 6 N glycine [56]. The discontinuous gels consisted of a 5 cm separating gel (16.5% tricine, 6% C w/6 N urea), 1 cm spacer gel (10% tricine, 3% C) and 1 cm stacking gel (4% tricine, 3% C), where 'C' refers to the bis-acrylamide content. Gels were stained with Coomassie blue [57] or silver stained [58]. The molecular weights of the peptides were determined using  $R_f$  measurements from molecular weight markers. In some cases peptides were also separated using 12.5% SDS-PAGE as described [34,57], based on the system of Laemmli [59].

### 2.7. Additional assays and analyses

Phosphate was determined as described [60] and modified [61]. Total protein was determined using a Bio-Rad microassay procedure (Sigma). The prediction of the secondary structure and the hydrophathy index of the individual peptides was derived on a Silicon graphics VGX workstation using a loop search technique with SYBYL. The secondary structure was predicted according to the method of Robson-Garnier [62] and the hydrophilicity plots calculated according to the algorithm of Hopp and Woods [63]. Hill plots were constructed and the Hill coefficient calculated as described [64]. In depolarization studies  $Y$  was defined as the percent fluorescence recovery. In the aggregation studies  $Y$  was defined as the change in absorbance at 380 nm. The slope of the plot of  $\log[\text{peptide concentration}]$  versus  $\log Y/[Y_{\text{total}} - Y]$  is equal to the Hill coefficient and was calculated using Sigma-plot linear regression software. The data were first analyzed using Sigma Stat to determine whether the best fit was a first or

Table 1  
Amino acid sequence of peripherin/rds peptides and a rhodamine labeled analogue

Designation	Sequence	Molecular weight (g/mole)
PP-5	H <sub>2</sub> N-VPETWKAFLESVKKL-COOH	1819.2
PP-5AB	H <sub>2</sub> N-VPETWKAYLESEKKL-COOH	1848.2
PP-5HB	H <sub>2</sub> N-VPETWPAFLESVKKL-COOH	1787.2
Rh-PP-5	Rho-HN-VPETWK*AFLESVK*K*L-COOH	2251.0
PP-3	H <sub>2</sub> N-VEAEGEDAGQAPAAG-COOH	1694.3
PP-2	H <sub>2</sub> N-RKRSVDMNNSDSHFV-COOH	1859.0

\* designates a trypsin cleavage site.

The amino acids indicated in bold are those residues altered in the mutant peptides.

second order equation, which was then used for Hill analysis.

### 3. Results

Photoreceptor peripherin/rds contains a candidate fusion peptide region within the C-terminus [33,34], corresponding to amino acids 311–325. A peptide representing this fusion domain (PP-5), two mutant peptides and several other peptides of overlapping regions of the C-terminus were synthesized and used in the following studies. The wild type (WT) peptide was fluorescently labeled at its N-terminus with rhodamine and used in self-assembly studies. The sequences, molecular weights, and the designations given these peptides are shown in Table 1.

#### 3.1. PP-5 depolarizes model membrane

To delineate how the fusion domain of peripherin/rds promotes membrane fusion and to provide additional support for the role of PP-5 as a fusion peptide region of peripherin/rds we investigated the ability of this peptide to perturb membrane structure. Membrane destabilization was inferred as an increase in fluorescence of the fluorophore, diS-C<sub>2</sub>-5, caused

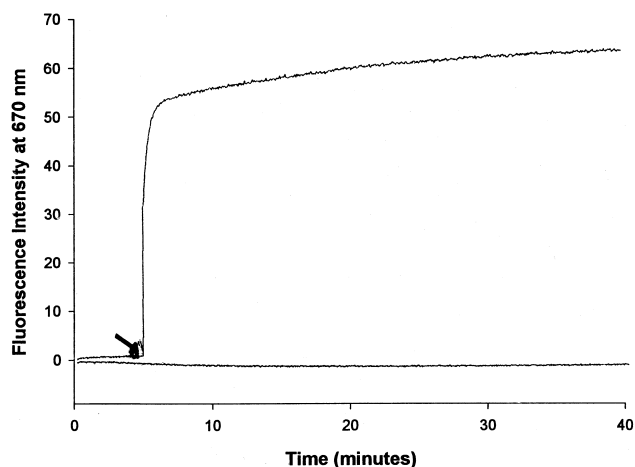


Fig. 1. PP-5 induced dissipation of valinomycin induced diffusion potential in phosphatidylcholine:phosphatidylserine:cholesterol SUVs. The fluorescence intensity of diS-C<sub>2</sub>-5, at  $\lambda_{\text{ex}} = 620$  nm and  $\lambda_{\text{em}} = 670$  nm was followed over time. The addition of PP-5 (concentration = 20  $\mu\text{g}$ ) to the vesicles containing valinomycin is shown by an arrow. The results shown are of a representative experiment.

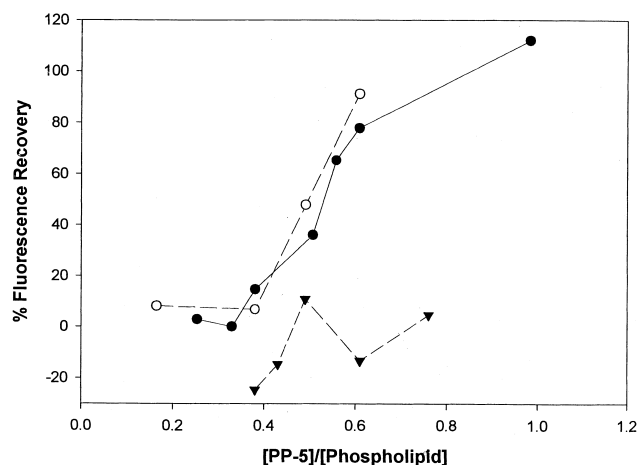


Fig. 2. Percent fluorescence recovery versus peptide to phospholipid (mole:mole) ratio. The maximum fluorescence recovery of diS-C<sub>2</sub>-5 at 37°C is plotted as a function of PP-5 to phospholipid molar ratios in samples containing PP-5 (●) alone, an equimolar mixture of PP-5 and PP-5HB (○), and an equimolar mixture of PP-5 and PP-5AB (▼). The results are a summary of two independent experiments with two different batches of PP-5.

by a dissipation of a valinomycin induced K<sup>+</sup> diffusion potential [65]. The ability of synthetic peptide analogues corresponding to the C-terminus of peripherin/rds, designated PP-3 to PP-7 corresponding to a 40 amino acid long region of the C-terminus (Table 1 and described previously [34]) to dissipate the valinomycin induced K<sup>+</sup> diffusion potential, was tested. An increase in diS-C<sub>2</sub>-5 fluorescence intensity occurred only when PP-5 was added to the valinomycin treated LUVs (Fig. 1). In contrast, the fluorescence intensity was unaltered with the addition of any of the other peptide analogues studied (PP-3 to PP-7, data not shown).

FTIR analysis of PP-5 showed that this peptide is an amphiphilic  $\alpha$ -helix in aqueous solution [34]. To investigate the effects of amphiphilicity and helical structure on PP-5 dependent aggregation, two mutant peptide analogues of PP-5, PP-5HB and PP-5AB, were designed to alter either the amphiphilic nature or the  $\alpha$ -helical structure of PP-5. PP-5AB differs from PP-5 at two amino acids, the first, F318Y and the second, V322E. These substitutions are designed to disrupt the segregated distribution of hydrophilic and hydrophobic residues within the peptide and are designated an amphiphilic breaker. These two amino acid substitutions result in a more

hydrophilic structure with a net charge of zero and an increase in the predicted hydropathy index. Model studies suggest that the  $\alpha$ -helical structure of this peptide is unaltered (data not shown). The other mutant peptide with a L316P substitution, called PP-5HB, is predicted by molecular modeling to have a disordered secondary structure (data not shown).

As seen in Fig. 2, increasing amounts of equimolar mixtures of PP-5 and PP-5 AB (relative to phospholipid) were unable to promote depolarization, suggesting that PP-5 induced depolarization is inhibited by PP-5AB. In contrast, when PP-5 and PP-5 HB were added simultaneously, in equimolar amounts, the diffusion potential dissipated to the same extent as that observed with PP-5 alone (data not shown).

### 3.2. Characterization of peptide oligomerization

A common characteristic of membrane fusion peptides is the formation of oligomeric complexes which act to promote the steps in fusion. The non-linear relationship between % depolarization and molar ratio of PP-5 suggests that PP-5 dependent depolarization is dependent on PP-5 oligomerization. To address the relationship between PP-5 function (depolarization) and its structure, the oligomeric forms of the peptides were characterized using discontinuous gel electrophoresis (summarized in Table 2). The most prevalent form of PP-5 under denaturing conditions is a complex with a molecular weight of 3600 indicative of a dimer. The apparent absence of PP-5 monomers is similar to other fusion peptides which form stable complexes in the presence of SDS [66] and denature only at extremely high temperatures. We have previously shown using FTIR that native peripherin/rds denatures at extremely high temperatures [33].

Under non-denaturing electrophoresis conditions, PP-5 migrated within an apparent molecular mass range of 6800–7200 Da, indicative of a tetramer. In the HPLC analysis, PP-5 eluted with an apparent molecular mass of 7500–8400 Da indicative of a tetramer with less than 10% corresponding to a dimer (Fig. 3A, peak A and B respectively). Analysis of the two mutant peptides, PP-5AB and PP-5HB, showed PP-5HB to be dimeric (Fig. 3B, peak C') and PP-5AB to form a tetramer and a trimer (Fig. 3B, peak A' and B' respectively). An equimolar mixture of PP-

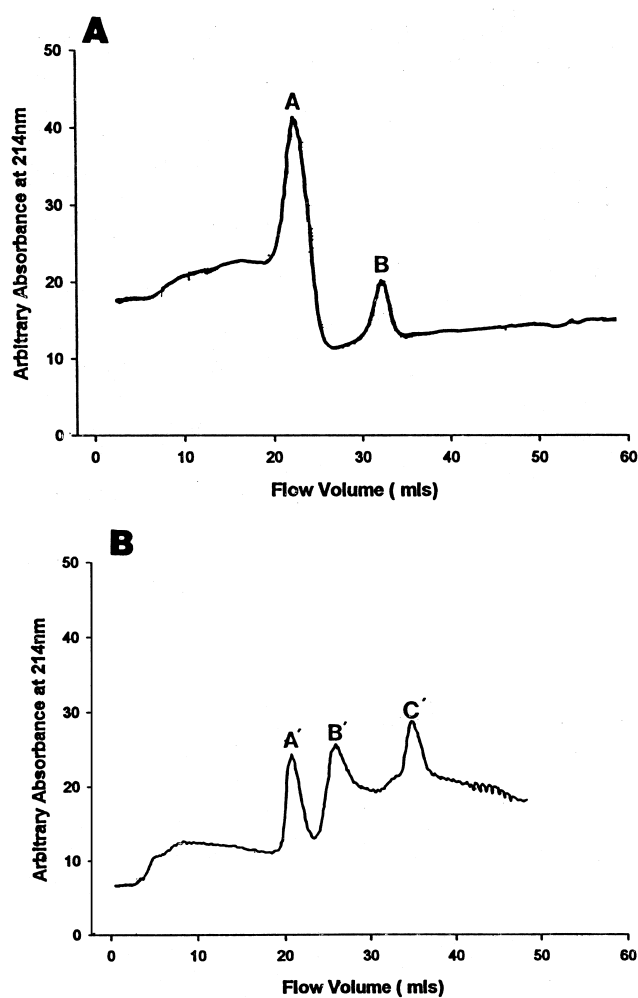


Fig. 3. Elution profile of PP-5 and mutant peptides. (A) The elution profile of PP-5 separated on a HR10/30 Superdex column eluted with an isocratic gradient of 0.25 M NaCl in 0.02 M  $\text{Na}_2\text{HPO}_4$  pH 7.40 at a flow rate of 0.25 ml/min was monitored at 214 nm. (B) The elution profile of an equimolar mixture of PP-5HB with PP-5AB under the same experimental conditions as in A. Peak assignments were based on individual runs of the various peptides and elution volumes of the standards as described in Section 2.

5 and PP-5AB formed a tetramer and a dimer (data not shown).

### 3.3. PP-5 self-assembly in the presence of SUVs

The data above demonstrating the presence of multiple oligomeric forms of PP-5 suggest the self-assembly of this peptide in solution. To gain additional support for PP-5 self-association, a rhodamine labeled analogue of PP-5 was synthesized (Table 1).



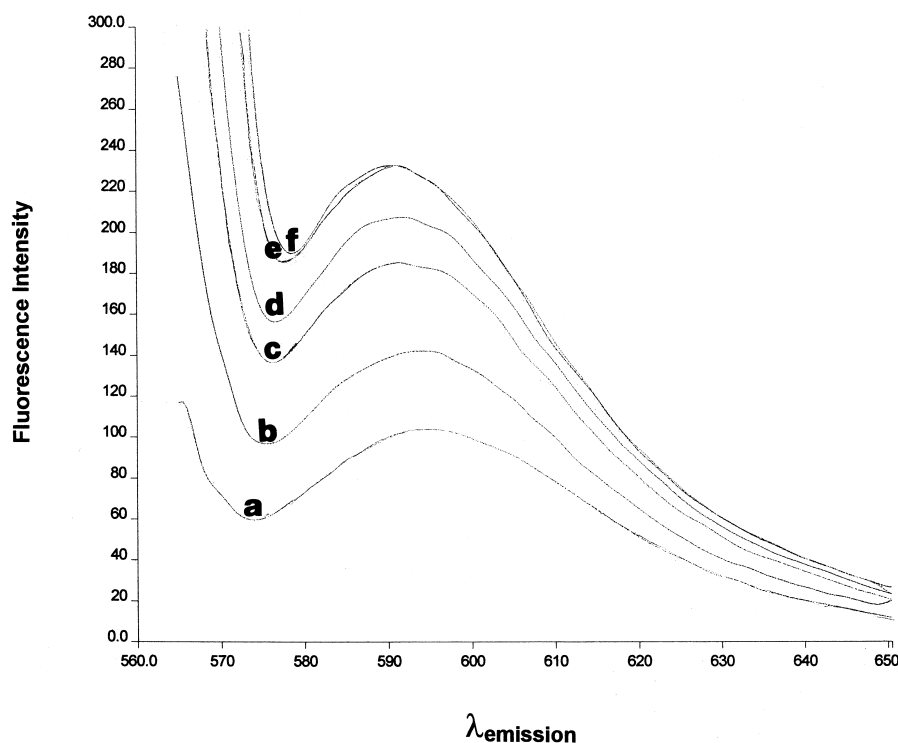


Fig. 4. Fluorescence emission spectra of RhPP-5 in the presence of increasing amounts of SUVs. The fluorescence emission spectra of 20 nM RhPP-5 from 560 to 650 nm at a  $\lambda_{\text{ex}} = 560$  nm is shown in buffer, (curve f) and in the presence of increasing amounts of PC:PS:CHOL (4:4:1) SUVs at 37°C (curves a–e). The phospholipid concentration in the assay during each scan is as follows: e, 25 nM; d, 130 nM; c, 0.25  $\mu\text{M}$ ; b, 0.52  $\mu\text{M}$ ; a, 0.77  $\mu\text{M}$ .

The fluorescence of RhPP-5 at  $\lambda_{\text{em}} = 586$  nm was monitored in an aqueous environment and in the presence of SUVs prepared exactly as described in the depolarization studies (i.e. PC:PS:CHOL 4:4:1). The emission spectra of RhPP-5 in aqueous solution reflected the fluorescence of the rhodamine

moiety with a decrease in intensity as the concentration of RhPP-5 was increased (data not shown). Similarly in the presence of lipid vesicles, when the amount of vesicles present in the assay was doubled, the fluorescence intensity at 586 nm decreased from 178 fluorescence units to 124 fluorescence units

Table 2  
Oligomeric complexes formed by peripherin/rds peptides

Peptides	Predicted oligomeric form		
	Denaturing conditions	Non-denaturing conditions	
		Gels	HPLC
PP-5	3 600 (dimer)	7 200(tetramer)	7 650(tetramer)
PP-5+PP-5HB	2 930 (dimer)	8 000(tetramer) 3 700(dimer)	7 800(tetramer)
PP-5+PP-5AB	4 660 (trimer, 98%)	7 200(tetramer)	7 850(tetramer)
	3 030 (dimer, 2%)	3 580(dimer)	3 500(dimer)
PP-5HB+PP-5AB	4 720 (trimer, 93%)	7 500(tetramer)	7 500(tetramer)
	3 190 (dimer, 6%)	15 000(octamer)	13 500(octamer)

The molecular weights of the various peptides were determined under denaturing and non-denaturing conditions as described in Section 2. The predicted oligomeric forms of the peptides given in parentheses are based on the molecular weights of the peptides shown in Table 1.

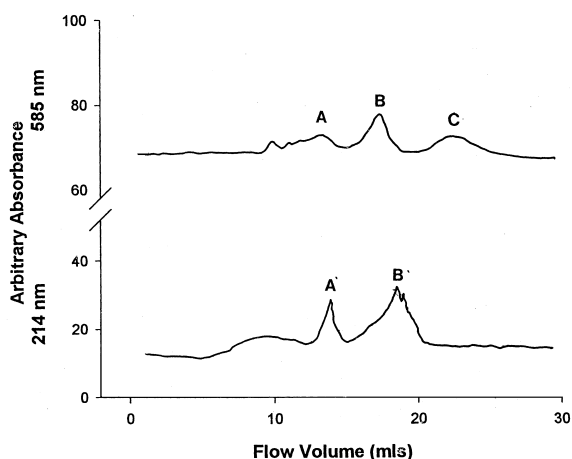


Fig. 5. Elution profile of equimolar mixtures of RhPP-5 and PP-5AB. The elution profile of an equimolar mixture of RhPP-5 with PP-5AB separated on a HR10/30 Superdex column eluted with an isocratic gradient of 0.25 M NaCl in 0.02 M  $\text{Na}_2\text{HPO}_4$  pH 7.40 at a flow rate of 0.50 ml/min was monitored at 585 nm and 214 nm. Peak C corresponds to a species with a molecular weight consistent with a rhodamine moiety in solution.

(curve c and b respectively, Fig. 4). The simplest interpretation for the decrease in fluorescence intensity is a self-quenching of the fluorescence probe as would occur during self-assembly [67].

The oligomeric forms of mixtures of RhPP-5 and PP-5 were analyzed using HPLC size exclusion chromatography with the eluate monitored at 585 nm to detect rhodamine labeled PP-5 and 214 nm to detect peptide. The chromatograms detected the presence of two molecular species with molecular masses of 8250 Da (peak A) and 3960 Da (peak B). Complexes of nearly identical molecular masses were detected in mixtures of RhPP-5 and PP-5AB at both wavelengths (Fig. 5, peaks A, B, A', B'), suggesting the formation of heterooligomers. Mixtures of RhPP-5 and PP-HB showed a rhodamine peak corresponding to a tetramer ( $A_{585\text{nm}}$ ) and a non-fluorescent peak ( $A_{214\text{nm}}$ ) corresponding to a dimer (data not shown) suggesting the formation of two different homooligomers, a RhPP-5 tetramer and a PP-5HB dimer.

### 3.4. PP-5 promotes vesicle aggregation

To determine whether the stoichiometry necessary for depolarization was also that necessary to promote vesicle aggregation (i.e. suggesting similar

mechanistic steps), we investigated the concentration dependence of PP-5 promoted vesicle aggregation [34]. As the ratio of PP-5 to lipid was increased, a non-linear relationship between concentration and extent of aggregation was observed (Fig. 6). Vesicle aggregation was markedly sensitive to PP-5, with aggregatory effects seen at a molar ratio of peptide to phospholipid equal to  $2.0 \times 10^{-3}$ . The relative amount of PP-5 required to promote aggregation is less than that previously shown to be necessary to promote model membrane fusion [34] or PP-5 dependent depolarization. In contrast to PP-5 mediated depolarization (Fig. 2), which is inhibited by PP-5AB, neither PP-5AB nor PP-5HB, in an equimolar concentration with PP-5, affected PP-5 induced vesicle aggregation (data not shown). Neither PP-5AB nor PP-5HB alone promoted vesicle aggregation at any concentration studied (data not shown), indicating that an amphiphilic  $\alpha$ -helix as seen in WT PP-5 is necessary for aggregation. These results show that PP-5 induced vesicle aggregation occurs at much lower molar ratio of peptide to phospholipid than PP-5 dependent depolarization (molar ratio of  $2.0 \times 10^{-3}$  versus molar ratio of 0.4, respectively). Moreover, only PP-5 induced membrane depolarization is susceptible to inhibition by PP-5AB.

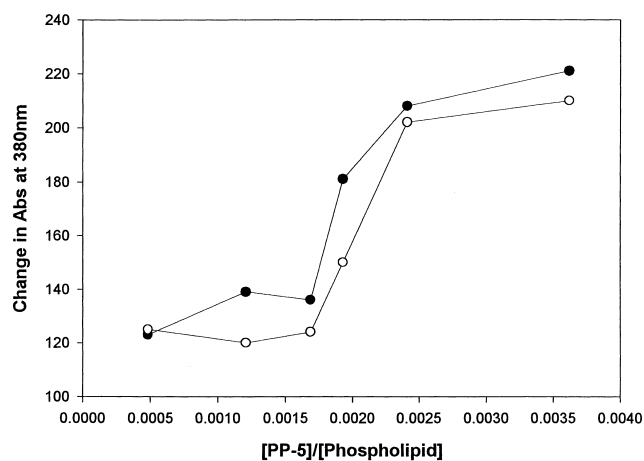


Fig. 6. PP-5 induced calcium dependent vesicle aggregation. The maximum change in absorbance at 380 nm of PC:PS:CHOL (4:4:1) vesicles in the presence of increasing concentrations of PP-5 (●) or equimolar mixtures of PP-5 and PP-5AB (○) is shown at 37°C. The calcium concentration in these assays was 16  $\mu\text{M}$  as described in Section 2. The results are a summary of two independent experiments with two different batches of PP-5.

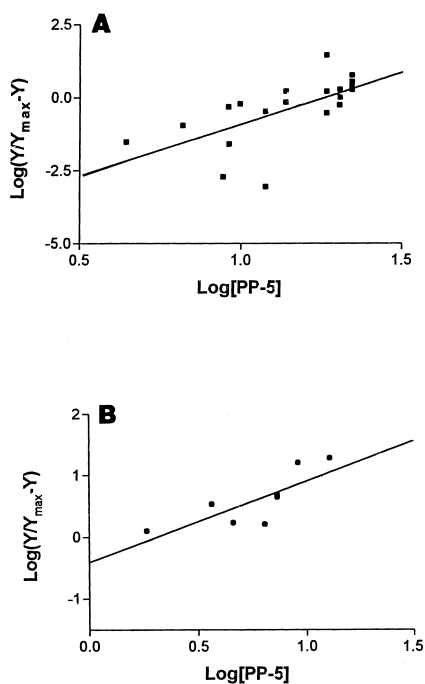


Fig. 7. Modified Hill analysis of aggregation and depolarization data. (A) Hill plot of  $\log[Y/(Y_{\max} - Y)]$  versus  $\log[\text{PP-5}]$  was constructed from the data shown in Fig. 2 and similar experiments ( $n=21$  data points).  $Y$  was defined as the percent fluorescence recovery and  $Y_{\max}$  the maximal percent recovery determined with the addition of mellitin. The slope of the plot of  $\log[\text{peptide concentration}]$  versus  $\log Y/[Y_{\max} - Y]$  is equal to the Hill coefficient and was calculated using Sigma-plot linear regression software. The data were first analyzed using Sigma Stat to determine whether the best fit was a first or second order equation. (B) Hill plot of  $\log[Y/(Y_{\max} - Y)]$  versus  $\log[\text{PP-5}]$  was constructed from the data shown in Fig. 6 and similar experiments ( $n=9$  data points).  $Y$  was defined as the absorbance at 380 nm and  $Y_{\max}$  the maximum absorbance at 380 nm. The slope of the plot of  $\log[\text{peptide concentration}]$  versus  $\log Y/[Y_{\max} - Y]$  is equal to the Hill coefficient and was calculated using Sigma-plot linear regression software.

### 3.5. Predicted effects of PP-5 oligomers on membrane aggregation and depolarization

The data in Figs. 2 and 6 show a qualitatively albeit not quantitatively similar non-linear relationship between membrane depolarization (Fig. 2) or vesicle aggregation (Fig. 6) and peptide/phospholipid ratio. Since oligomeric complexes of PP-5 were present under non-denaturing conditions we wished to learn whether these higher order oligomeric complexes of PP-5 accounted for the apparent dose re-

sponse seen in the aggregation and depolarization data. Therefore, the data in Figs. 1 and 6 were analyzed using a modified Hill analysis (Fig. 7A,B). The slope of the plot of  $\log[\text{PP-5}]$  versus  $\log[Y/(Y_{\max} - Y)]$  for membrane depolarization (i.e. the Hill coefficient) was equal to 3.725 (Fig. 7A), suggesting that PP-5 may form a tetrameric or higher order oligomer to promote depolarization. In contrast to membrane depolarization, when the PP-5 induced vesicle aggregation data (Fig. 1) were similarly analyzed (Fig. 7B), the slope of the plot was calculated to be 1.324, suggesting that PP-5 self-assembly may not be required for aggregation.

## 4. Discussion

We have previously provided evidence supporting the hypothesis that peripherin/rds is a photoreceptor specific membrane fusion protein [33,34]. A fusion peptide region of this protein has been identified within the C-terminus, corresponding to amino acid residues 311–325. This region is modeled by a synthetic peptide, termed PP-5, which has previously been shown to promote membrane aggregation and fusion, as measured by aqueous contents mixing [34]. The present study extends our characterization of PP-5 by showing that PP-5 promotes membrane depolarization, and by inference membrane destabilization. In addition, other synthetic peptides corresponding to overlapping regions within the C-terminus of peripherin/rds (from amino acid residues 308 to 345) did not promote membrane aggregation [34], aqueous contents mixing [34] or depolarization (results presented herein). These observations provide additional support for a specificity of a fusion peptide region within amino acids 311–324.

The salient observation in this study is that membrane depolarization and by inference membrane destabilization require an oligomer of PP-5. A tetrameric complex of PP-5 was detected in both size exclusion chromatography experiments (Fig. 4A and B, Table 2) and non-denaturing tricine gel electrophoresis (Table 2). In addition, self-assembly of PP-5 into multimeric complex was demonstrated using RhPP-5, in the presence of vesicles of identical size and composition as in the depolarization studies. Cooperativity was reinforced with a Hill analysis of

the depolarization data, which resulted in a calculated slope of the Hill plot equal to 3.754 (Fig. 7A), suggesting that a tetrameric arrangement of PP-5 monomers may be required for maximal depolarization and by inference destabilization but not aggregation (Fig. 7B).

The amphiphilic  $\alpha$ -helical structure of PP-5 is a common feature of other fusion peptides [68,69]. To elucidate the relationship between PP-5 structure and function, two mutant peptides which altered the amphiphilic nature of the  $\alpha$ -helix of PP-5 (PP-5AB) or the  $\alpha$ -helical structure (PP-5HB) were studied. Interestingly, PP-5HB had no effect on PP-5 dependent depolarization, but PP-5AB inhibited PP-5 dependent membrane depolarization. An understanding of the action of PP-5AB and by inference wild type PP-5 can be obtained from an analysis of the properties of PP-5 and PP-5AB and PP-5HB. The mutant peptide PP-5AB inhibited PP-5 induced membrane depolarization. The mechanism of PP-5AB inhibitory action appears to be via the formation of a non-functional heterotetrameric complex. Experiments using rhodamine labeled PP-5 (Figs. 4 and 5) and PP-5AB detected a dimer and a tetramer at both  $A_{214\text{nm}}$  (peptide absorbance) and at  $A_{585\text{nm}}$  (rhodamine absorbance). Because the molecular mass of the larger species (8200 Da) detected at both absorbances is exactly that predicted from an arithmetic sum of the molecular masses of two rhodamine PP-5s and two PP-5ABs, it can be concluded that a heterotetramer, rather than a homotetramer, is the dominant species present. If a PP-5 AB homotetramer was present then an additional peak at  $A_{214\text{nm}}$  would have been detected with a molecular mass of 3700 Da (between peaks A and B in Fig. 5), with no corresponding peak observed at  $A_{585\text{nm}}$ . PP-5AB inhibition of PP-5 dependent action suggests that the PP-5-PP-5AB heterotetramer does not induce depolarization (Fig. 3). Since PP-5 and PP-5AB form a heterotetramer it can be inferred that amphiphilicity is not required for complex formation. In studies of peptides of HA2, the elimination of the amphiphilic characteristic abolished fusion due to a disruption of the  $\alpha$ -helical structure [69]. In contrast, when the amphiphilic nature of the  $\alpha$ -helix in the WAE model peptide was altered an increase in fusion activity was observed [70]. However, in neither one of those stud-

ies was the oligomeric state of the peptides investigated. More recently, work with a net negative amphiphilic peptide has shown that this peptide must be anchored to liposomes to promote fusion [71]. Such studies remain to be carried out with PP-5.

In contrast to PP-5AB, PP-5HB formed a disordered secondary structure which had no effect on PP-5 dependent membrane depolarization or vesicle aggregation (Fig. 2 and data not shown). Equimolar mixtures of PP-5 and PP-5HB formed dimers and tetramers with an unknown molecular stoichiometry within these complexes. Since PP-5 HB does not inhibit membrane depolarization, it can be inferred that PP-5HB forms homodimers and PP-5 forms homotetramers in these mixtures. Thus, PP-5HB does not prevent the self-assembly of PP-5 to a homotetramer. This interpretation is confirmed by Hill analysis of depolarization data using PP-5-PP-5HB, in which the Hill coefficient was approx. 4 indicating that the depolarization competent species was most likely a PP-5 homotetramer.

The hypothesis that the fusion peptide of peripherin/rds modeled by PP-5 forms oligomers which are necessary for membrane depolarization is consistent with other fusion peptides [2–4], lending additional support for the role of this region of the native protein in promoting membrane fusion. This hypothesis is also consistent with our previously published work reporting an inhibition of fusion between R<sub>18</sub> labeled ROS plasma membrane and peripherin/rds recombinants by PP-5. In those experiments it is proposed that the inhibition of fusion results from the interaction of PP-5 with its corresponding region in native peripherin/rds. Such an interaction may result in improper self-assembly of the native protein. The formation of a higher order oligomeric complex by native peripherin/rds was also documented using sedimentation analysis [44]. The precise stoichiometry of the fusion competent form of native peripherin/rds remains to be determined. The demonstration that PP-5 promotes membrane depolarization and membrane aggregation provides additional and more compelling support for its role in ROS membrane fusion processes and the identification of this region of native peripherin/rds as a fusion peptide domain.

## Acknowledgements

The authors would like to thank Michael Santilli for his expert technical assistance and Dr. R. Schimmel and Dr. J. Lenard for their critical reading of the manuscript. This work was supported by NIH EY10420, with an NIH Minority Supplement to MF, and by a UMDNJ-GSBS-Summer Undergraduate Research Fellowship to AAN.

## References

- [1] N. Duzgunes, in: D. Roodyn (Ed.), *Subcellular Biochemistry*, Plenum Press, London, 1985, p. 195.
- [2] L.D. Hernandez, L.R. Hoffman, T.G. Wolfsberg, J.M. White, *Annu. Rev. Cell Dev. Biol.* 12 (1996) 627–661.
- [3] El. Pescher, J. SainteMarie, A. Bienvenue, D. Hoekstra, *J. Membr. Biol.* 167 (1999) 1–17.
- [4] C.P. Blobel, T.G. Wolfsberg, C.W. Turck, D.G. Myles, P. Primakoff, J. White, *Nature* 356 (1992) 248–252.
- [5] W.J. Snell, J. White, *Cell* 85 (1996) 629–637.
- [6] T.G. Wolfsberg, P. Primakoff, D.G. Myles, J. White, *J. Cell Biol.* 131 (1995) 275–278.
- [7] T.G. Wolfsberg, J.M. White, *Dev. Biol.* 180 (1996) 389–401.
- [8] J. White, *Science* 258 (1992) 917–924.
- [9] S. Takahashi, *Biochemistry* 29 (1990) 6257–6264.
- [10] C. Harter, P. James, T. Bachi, G. Semenza, J. Brunner, *J. Biol. Chem.* 264 (1989) 6459–6464.
- [11] R. Brasseur, M. Vandenbranden, B. Cornet, A. Burny, J.M. Ruyschaert, *Biochim. Biophys. Acta* 1029 (1990) 267–273.
- [12] M. Horth, B. Lambrecht, M. Chuah, L. Khim, F. Bex, C. Thiriart, J.-M. Ruyschaert, A. Burny, R. Brasseur, *EMBO J.* 10 (1991) 2747–2755.
- [13] A. Muga, W. Neugebauer, T. Hiram, W.T. Surewicz, *Biochemistry* 33 (1994) 4444–4448.
- [14] I. Martin, R.M. Epand, J.M. Ruyschaert, *Biochemistry* 37 (1998) 17030–17039.
- [15] T. Stegmann, R.W. Doms, A. Helenius, *Annu. Rev. Biophys. Biophys. Chem.* 18 (1989) 187–211.
- [16] M. Tsurudome, R. Gluck, R. Graf, R. Falchetto, U. Schaller, J. Brunner, *J. Biol. Chem.* 267 (1992) 20225–20232.
- [17] C.C. Pak, M. Krumbiegel, R. Blumenthal, Y. Raviv, *J. Biol. Chem.* 269 (1994) 14614–14619.
- [18] R.W. Ruigrok, A. Aitkin, L.J. Calder, S.R. Martin, J.J. Skehel, S.A. Wharton, W. Weis, D.C. Wiley, *J. Gen. Virol.* 69 (1988) 2785–2795.
- [19] S.A. Wharton, S.R. Martin, R.W. Ruigrok, J.J. Skehel, D.C. Wiley, *J. Gen. Virol.* 69 (1988) 1847–1857.
- [20] T. Stegmann, I. Bartoldus, J. Zumbur, *Biochemistry* 34 (1995) 1825–1832.
- [21] F.M. Hughson, *Curr. Biol.* 5 (1995) 265–274.
- [22] H.R. Guy, S.R. Durell, C. Schoch, R. Blumenthal, *Biophys. J.* 62 (1992) 95–97.
- [23] T. Danieli, S.L. Pelletier, Y.I. Henis, J. White, *J. Cell Biol.* 133 (1996) 559–569.
- [24] R.W. Young, *Invest. Ophthalmol. Vis. Sci.* 15 (1976) 700–710.
- [25] J.R. Currie, J.G. Hollyfield, M. Rayborn, *Vis. Res.* 18 (1978) 995.
- [26] J.M. Corless, M.J. Costello, *Exp. Eye Res.* 32 (1981) 217–228.
- [27] J.C. Besharse, D.A. Dunis, in: *The Structure of the Eye*, Elsevier, New York, 1982, p. 85.
- [28] J.M. Corless, R.D. Fetter, *J. Comp. Neurol.* 257 (1987) 24.
- [29] A.M. Laties, D. Bok, P. Liebman, *Exp. Eye Res.* 23 (1976) 139–148.
- [30] B. Matsumoto, J.C. Besharse, *Invest. Ophthalmol. Vis. Sci.* 26 (1985) 628–635.
- [31] J.C. Besharse, G. Hageman, *Invest. Ophthalmol. Vis. Sci.* 31 (1990).
- [32] K. Boesze-Battaglia, A.D. Albert, P.L. Yeagle, *Biochemistry* 31 (1992) 3733–3737.
- [33] K. Boesze-Battaglia, F. Kong, O.P. Lamba, F.P. Stefano, D.S. Williams, *Biochemistry* 36 (1997) 6835–6846.
- [34] K. Boesze-Battaglia, O.P. Lamba, A.A. Napoli, S. Sinha, Y. Guo, *Biochemistry* 37 (1998) 9477–9487.
- [35] K. Boesze-Battaglia, *Invest. Ophthalmol. Vis. Sci.* 38 (1997) 487–497.
- [36] K. Arikawa, L. Molday, R.S. Molday, D.S. Williams, *J. Cell Biol.* 116 (1992) 659–667.
- [37] R.S. Molday, D. Hicks, L. Molday, *Invest. Ophthalmol. Vis. Sci.* 28 (1987) 50–60.
- [38] G.H. Travis, M.B. Brennan, P.E. Danielson, C.A. Kozak, J.G. Sutcliffe, *Nature* 338 (1989) 70–73.
- [39] G. Connell, R.S. Molday, *Biochemistry* 29 (1990) 4691–4698.
- [40] W. Kedzierski, W.N. Moghrabi, A.C. Allen, M.M. Jablonski-Stiemke, S.M. Azarian, D. Bok, G. Travis, *J. Cell Sci.* 109 (1996) 2551–2560.
- [41] A.F.X. Goldberg, L. Moritz, R.S. Molday, *Biochemistry* 34 (1995) 14213–14219.
- [42] A.F.X. Goldberg, R.S. Molday, *Biochemistry* 35 (1996) 6144–6149.
- [43] A.F.X. Goldberg, R.S. Molday, *Proc. Natl. Acad. Sci. USA* 93 (1996) 13726–13730.
- [44] R.S. Molday, C.J. Loewen, L. Molday, *Invest. Ophthalmol. Vis. Sci.* 39, 4 S11 (1998) 45.
- [45] G.H. Travis, J.G. Sutcliffe, D. Bok, *Neuron* 6 (1991) 61–70.
- [46] W.R. Gallagher, *Cell* 50 (1987) 327–328.
- [47] J.M. White, *Annu. Rev. Physiol.* 52 (1990) 675–697.
- [48] D. Rappaport, Y. Shai, *J. Biol. Chem.* 269 (1994) 15124–15131.
- [49] S.A. Monsma, G.W. Blissard, *J. Virol.* 69 (1995) 2583–2595.
- [50] R. Epand, J.J. Cheetham, R.F. Epand, P.L. Yeagle, C.D. Richardson, A. Rockwell, W.F. De Grado, *Biopolymers* 32 (1992) 309–314.
- [51] F.A. Rey, F.X. Heinz, C. Mandl, C. Kunz, S.C. Harrison, *Nature* 375 (1995) 291–298.

- [52] A. Muga, W. Neugebauer, T. Hirma, W.K. Surewicz, *Biochemistry* 33 (1994) 4444–4448.
- [53] Y. Kliger, A. Aharon, D. Rapaport, P. Jones, R. Blumenthal, Y. Shai, *J. Biol. Chem.* 272 (1997) 13496–13505.
- [54] G. Schwarz, S. Stankowski, V. Rizzo, *Biochim. Biophys. Acta* 861 (1986) 141–151.
- [55] E. Gazit, Y. Shai, *Biochemistry* 32 (1993) 12363–12371.
- [56] H. Schagger, G. Von Jagow, *Anal. Biochem.* 166 (1987) 368–379.
- [57] H.G. Smith, G.W. Stubbs, B.J. Litman, *Exp. Eye Res.* 20 (1975) 211–217.
- [58] C.R. Merrill, D. Goldman, M.L. Van Keuran, *Electrophoresis* 3 (1982) 17–23.
- [59] U.K. Laemmli, *Nature* 227 (1970) 680–685.
- [60] G.R. Bartlett, *J. Biol. Chem.* 234 (1959) 466–473.
- [61] B.J. Litman, *Biochemistry* 13 (1973) 2545–2554.
- [62] Garnier, Osguthorpe, Robson, *J. Mol. Biol.* 120 (1978) 97–102.
- [63] Hopp, Woods, *Proc. Natl. Acad. Sci. USA* 78 (1981) 3824–3828.
- [64] K.E. Neet, in: D.L. Purich (Ed.), *Methods in Enzymology*, vol. 249: *Enzyme Kinetics and Mechanisms*, Academic Press, San Diego, CA, 1995.
- [65] L.M. Loew, I. Rosenberg, M. Bridge, C. Gitler, *Biochemistry* 22 (1983) 837–844.
- [66] T. Hayashi, H. McMahon, S. Yamasaki, T. Binz, Y. Hata, T.C. Sudhof, H. Niemann, *EMBO J.* 13 (1994) 5051–5061.
- [67] P.M. Keller, S. Person, W. Snipes, *J. Cell Sci.* 28 (1977) 167–180.
- [68] R. Ishiguro, M. Matsumoto, S. Takahashi, *Biochemistry* 35 (1996) 4976–4982.
- [69] S. Takahashi, *Biochemistry* 29 (1990) 6257–6264.
- [70] E.I. Pecheur, D. Hoekstra, J. Sainte-Marie, L. Maurin, A. Bienvenue, J.R. Phillipot, *Biochemistry* 36 (1997) 3773–3781.
- [71] E.-I. Pecheur, I. Martin, J.M. Ruyschaert, A. Bienvenue, D. Hoekstra, *Biochemistry* 37 (1998) 2361–2371.